Biodegradation efficiencies and economic feasibility of single-stage and two-stage anaerobic digestion of desulfated Skim Latex Serum (SLS) by using rubber wood ash

Marisa Raketh, Prawit Kongjan, Khaliyah Sani, Eric Trably, Benjamas Cheirsilp, Rattana Jariyaboon

Biodegradation Efficiencies and Economic Feasibility of Single-stage and Two-Stage Anaerobic Digestion of Desulfated Skim Latex Serum (SLS) by Using Rubber Wood Ash

Marisa Raketh[1,3], Prawit Kongjan[2,3], Khaliyah Sani[1,3], Eric Trably[4], Benjamas Cheirsilp[5], Rattana Jariyaboon[2,3,*]

[1] Energy Technology Program, Faculty of Engineering, Prince of Songkla University, Hat Yai, Songkhla, 90112, Thailand

[2] Department of Science, Faculty of Science and Technology, Prince of Songkla University (PSU), Pattani, 94000, Thailand

[3] Bio-Mass Conversion to Energy and Chemicals (Bio-MEC) Research Unit, Faculty of Science and Technology, Prince of Songkla University (PSU), Pattani, 94000, Thailand

[4] INRAE, Univ Montpellier, LBE, Narbonne, France

[5] Biotechnology for Bioresource Utilization Laboratory, Department of Industrial Biotechnology, Faculty of Agro-Industry, Prince of Songkla University, Hat-Yai, Songkhla 90112, Thailand

*corresponding author at: Department of Science, Faculty of Science and Technology, Prince of Songkla University (PSU), Pattani 94000, Thailand. Tel.: +66 73 313928-50 ext1988, mobile: +66 808721260.

E-mail address: rattana.sa@psu.ac.th (R. Jariyaboon).

ABSTRACT

The efficiencies of single-stage anaerobic digestion (SSAD) and two-stage anaerobic digestion (TSAD) of desulfated skim latex serum (DSLS) using various rubber wood ash (RWA) loadings were investigated in this study. The experiments on batch processes showed that DSLS gave a higher yield (6-21%) than raw SLS in both SSAD and TSAD. The highest H_2 and CH_4 yields of 90.64 and 294.53 mL/g-COD_{added} were achieved with DSLS using RWA loading of 5 g/L (DSLS5) and 10 g/L (DSLS10), respectively in TSAD (thermophilic and mesophilic conditions, respectively). The maximum 305.09 mL/g-COD_{added} CH_4 yield in SSAD was observed for DSLS10. Total energy recovery in TSAD was 5% higher than that in SSAD. However, the cost assessment on continuous AD using kinetics and yield from the batch experiments suggests longer payback time for TSAD (4.36 years) than for SSAD (2.52 years). TSAD is not economically attractive with DSLS10 due to the large total volume of digestors required. This study revealed that RWA can remove sulfate from SLS to enhance biogas production and reduces H_2S in the biogas, while TSAD of DSLS was not attractive compared to the conventional SSAD like for some other substrates reported in the literature.

Keywords: Skim Latex Serum, Two-stage anaerobic digestion, Bio-hydrogen, Bio-methane, Cost assessment

1. Introduction

Thailand is the main producer and exporter of several intermediate rubber products, such as concentrated latex, block rubber, and ribbed smoked sheet rubber. Concentrated latex is mainly produced with annual generation capacity of around 1.1 million tons from concentrated rubber latex plants, which are largely located in southern peninsular Thailand in 2020 (Rubber Intelligence Unit of Thailand, 2020).

When the fresh latex (with about 30% rubber content) is centrifuged, the main product of concentrated latex (with about 60% rubber content) is collected along with the skim latex by-product (with about 5% rubber content) (Danwanichakul et al., 2019). In skim latex process, sulfuric acid is added to precipitate and coagulate the rubber (Chaiprapat et al., 2015) and the wastewater from this process is called skim latex serum (SLS). It contains a large amount of sulfate (7500 mg/L), has high chemical oxygen demand (COD) (42.50 g/L), Volatile Solids (VS) (37.94), and low pH (5.51) (Raketh et al., 2021). The sulfate content in SLS can be converted to hydrogen sulfide under anaerobic conditions, which causes odor problems nearby the mill and has become a serious issue for latex rubber factories. Therefore, treatment of this wastewater before discharge to environment is crucial, otherwise it may cause water, air, and even soil pollution.

Anaerobic digestion (AD) is one of a number of techniques for treating SLS. Nonetheless, the high sulfate content in SLS could inhibit methanogens, resulting uncertain AD process with possibly low biogas yield (Jariyaboon et al., 2015). In our previous research work, rubber wood ash (RWA) was used to reduce sulfate in SLS with 42% sulfate removal efficiency, and the results indicated that RWA can reduce sulfate, with adsorption possibly as the main mechanism of sulfate removal, and the desulfated

SLS had improved biogas production (Raketh et al., 2021)

There are four steps in the AD process namely hydrolysis, acidogenesis, acetogenesis, and methanogenesis (Wang et al., 2020). The conventional AD process is performed in a single digester and is called single-stage AD (SSAD); it focuses on methane production. Actually, hydrogen is produced during acidogenesis and converted to methane during methanogenesis. Two-stage AD (TSAD) has been proposed to recover hydrogen in the first separated digestor and the effluent is fed to the second tank for further digestion. Split of TSAD to two reactor tanks allows optimizing hydrolysis/acidogenesis and methanogenesis and could enhance the overall reaction rate, maximize biogas yields, and create a process that is easier to control, both in meso- and thermophilic states (Schievano et al., 2012).

Many studies have shown that TSAD gives a higher overall degradation efficiency, and several authors have reported different applications of TSAD, with various organic substrates and different process designs .Sani et al. (2021) reported a comparative evaluation of SSAD and TSAD using palm oil mill effluent. The yield 264.73 mL-CH_4/g-COD_{added} was achieved in SSAD and 106.13 mL-H_2/g-COD_{added} and 334.56 mL-CH_4/g-COD_{added} were produced in TSAD. A 38.95% higher total energy fuel yield was found for TSAD compared to SSAD. Similar results were found when wheat feed pellets (Massanet-Nicolau et al., 2013) and poplar wood (Akobi et al., 2016) were used as substrates in a comparison study of SSAD and TSAD. Furthermore, food waste was used as substrate in TSAD yielding 20 and 18% more total energy than in SSAD, in the studies of De Gioannis et al. (2017) and Nathao et al. (2013), respectively. Conversely, there is a case reporting no significant differences in overall energy recovery between TSAD and SSAD systems using a mixture of swine manure and

97 market biowaste as substrate (Schievano et al., 2012). This result suggested the
98 hypothesis that the TSAD systems may in some cases bring no advantage in terms of
99 overall energy recovery yields.

100 The objective of the present study was to investigate whether TSAD of raw SLS
101 and desulfated SLS could generate more energy than SSAD. Moreover,
102 biodegradability, kinetics and cost assessments of both processes were also explored.

103

104 **2. Materials and methods**

105 2.1. Substrate and inoculum

106 Fresh raw SLS was collected from skim latex serum coagulation baths of the
107 concentrated latex factory in Songkhla province, Thailand. The main characteristics of
108 raw SLS and desulfated SLS (DSLS) with the level of RWA loading at 5, 10, 15, 20, and
109 30 g/L, are presented in Table 1. The SLS collected was stored at 4°C until use to
110 minimize self-biodegradation and acidification (the maximum storage time was 1
111 month).

112

113 **Table 1** Some characteristics of substrate and inoculum in AD process.

Parameters	**Substrate**						**Inoculum**	
	Raw SLS	**DSLS5**	**DSLS10**	**DSLS15**	**DSLS20**	**DSLS30**	**H_2**	**CH_4**
RWA loading (g/L)	0	5	10	15	20	30	-	-
pH	5.51	6.46	6.83	7.04	7.49	8.26	4.81	7.88
TS (g/L)	44.74	45.31	45.99	46.67	47.36	47.70	62.64	61.19
VS (g/L)	37.94	38.70	38.85	39.00	39.15	39.23	45.23	39.43
Ash (g/L)	6.8	6.99	7.85	8.72	9.58	10.01	17.41	21.76
COD (g/L)	43.11	42.69	42.88	43.07	43.26	43.36	NA	NA
Alkalinity (mg-$CaCO_3$/L)	3,287	3,318	3,336	3,656	3,787	4,101	NA	NA

Sulfate (mg/L)	7,500	5,200	4,250	4,900	6,150	6,500	NA	NA
TOC (g/L)	14.25	NA	NA	NA	NA	NA	NA	NA
TKN (mg/L)	1,548	NA	NA	NA	NA	NA	NA	NA

NA denoted not analyzed

RWA was collected from the high-pressure steam boiler of a glove factory in Songkhla province, Thailand. The main components in RWA were Ca and Si at 21.83 and 10.53 %w/w. K, S, Cl, Mg, and Fe were found in smallish amounts (6.43, 5.77, 3.15, 2.05, and 1.49 %w/w respectively) while some heavy metals were also observed as presented in our previous study (Raketh et al., 2021).

The mesophilic methane inoculum was obtained from the biogas plant of Phasaeng Green Power Co., Ltd., Surat Thani Province, Thailand, in which palm oil mill effluent was used as a substrate. The thermophilic inoculums for hydrogen production were prepared by shock loading the mesophilic methane inoculum using 50 g/L brown sugar in 800 mL working volume serum bottle to enrich hydrogen production bacteria. Then the serum bottles were closed with bottle caps and purged with nitrogen gas at a flow rate of 1 L/min for 3 min to ensure anaerobic conditions before incubation at 55 ºC afterwards. Daily biogas volume was measured by water displacement method while H_2, CO_2, and CH_4, concentrations in the biogas were analyzed by gas chromatography. The sugar in the same dosage was added into the shock-loaded inoculum for another acclimation. The CH_4 gas was detected only in the first day of first round acclimation, after that CH_4 gas no longer appeared. The hydrogen yield of shock-loaded inoculum in 3 rounds of acclimation were 63.76, 86.90, and 89.03 mLH_2/g-COD, respectively, then it was further used as inoculum for hydrogen production in two-stage anaerobic digestion (H_2-TSAD). Some characteristics of hydrogen and

methane inocula used in AD process are shown in Table 1.

2.2. Removal of sulfate from SLS

The rubber wood ash (RWA) levels of 5, 10, 15, 20, and 30 g/L were added to 1 L SLS before continuous stirring with a magnetic stirrer at a speed of 150 rpm for 10 minutes. After 10 minutes of mixing, the ash residue was immediately separated from mixed suspensions and the desulfated SLS was then used as a substrate for anaerobic digestion. The characteristics of solutions before and after adding RWA were analyzed in terms of pH and sulfate.

2.3. Biohydrogen and biomethane production in batch process

H_2-TSAD was carried out in 120 mL serum bottle with a working volume of 60 mL. Raw SLS and desulfated SLS (DSLS) with various initial solid loadings of RWA (5, 10, 15, 20, and 30 g/L) were used as substrate at initial loading of 28 g-COD/L and 70:30% v/v of substrate to inoculum ratio was added into each serum bottle (Angelidaki and Sanders, 2004; Kongjan et al., 2018) and adjusted to pH 7.0 with $NaHCO_3$. After that, the serum bottles were closed with bottle caps and purged with nitrogen gas at a flow rate of 1 L/min for 3 min to ensure anaerobic conditions before incubation at 55 ºC. The pH, sulfate, and volatile free fatty acids (VFAs) of effluent were investigated afterwards.

The effluents from the first stage of H_2-TSAD were used to determine methane production of two-stage anaerobic digestion (CH_4-TSAD), while Raw SLS and DSLS corresponding to 8.5 g-COD/L initial loading were used to determine methane production of single-stage anaerobic digestion (CH_4-SSAD). The procedure of CH_4-

159 TSAD and CH_4-SSAD experiments was as follows. First 60 mL of substrate was mixed
160 with a 140 mL methane inoculum in 500 mL serum bottle, leaving a 300 mL headspace.
161 The 70% by volume inoculum in the methane production stage was chosen to ensure
162 sufficient microorganisms for biomethane production potential (BMP) protocol
163 (Angelidaki and Sanders, 2004). A portion of wastewater was replaced by DI water for
164 blank control. The serum bottle was then closed with a bottle cap and purged with
165 nitrogen gas at a flow rate of 1 L/min for 3 min to ensure anaerobic conditions before
166 incubation at 35 ºC. The pH and sulfate of effluent were investigated afterwards.
167 All experiments were carried out in triplicate. Daily biogas volume was
168 measured by water displacement method while CH_4, H_2 CO_2, and H_2S concentrations in
169 the biogas were analyzed by gas chromatography. The fermentation was stopped when
170 no significant gas production was observed. The initial characteristics in H_2-TSAD and
171 CH_4-SSAD assay are shown in Table 2.
172
173 **Table 2** Conditions and initial main characteristics of H_2-TSAD and CH_4-SSAD

Parameter	**H_2-TSAD**	**CH_4-SSAD**
Working volume (mL)	60	200
TOC (g/L)	9.50	2.85
TKN (g/L)	1032	309
Alkalinity (g/L)	2191	657
Ash (g/L)	4.53	1.36
TS (g/L)	29.38	8.95
VS (g/L)	25.29	7.59
COD (g/L)	28.33	8.50

174
175
176 2.4. Analytical methods

The biogas production volume was measured through water displacement method. Hydrogen content in biogas was measured using gas chromatography (GC) (Shimadzu GC 14A, Shimadzu Corp., Kyoto, Japan), equipped with a stainless-steel column (2 m) packed with molecular sieve 58 (80/100 mesh) and equipped with a thermal conductivity detector (TCD). Each sample of biogas (0.5 mL) was injected into the GC with argon as the carrier gas at a flow rate of 35 mL/min. The GC column, injection port, oven, and detector were all set at 100 °C temperature. Methane, carbon dioxide, and hydrogen sulfite contents in biogas were also measured using gas chromatography (Shimadzu GC 14A equipped with a thermal conductivity detector), but with a 2.5 m Porapak S column with Hayesep Q (80/100). Helium was used as the carrier gas at a flow rate of 30 mL/min. The injection port, oven, and detector were set at 100, 60, and 110ºC respective temperatures. An 0.5 mL sample of the gas was injected in triplicate. VFAs were analyzed by gas chromatograph equipped with a flame ionization detector (GC-FID) (Shimadzu GC 8A). The column capillary was packed with fused silica and had 30 m length (Stabiwax® column). The GC-FID was equipped with an autosampler and an integrator. The chromatography used this program sequence: 60 °C for 35 min, 2 °C/min to 110 °C, 10 °C/min to 200 °C, and hold 1 min. The inlet and detector temperatures were set at 230° and 250°C, respectively.

The procedures described in the standard methods (APHA, 2012) were applied to determine pH, COD, TKN, total alkalinity, TS, VS, ash, and sulfate. TOC was investigated with TOC-Liquid: multi N/C 3100 TOC analyzer (Analytik Jena). Statistically significant differences in the results were determined using one-way analysis of variance (ANOVA) in SPSS v26.0 (IBM, USA).

201 2.5 Kinetic model analysis for TSAD and SSAD processes

202 Models for explaining the complex metabolic processes and predicting the
203 kinetics in the AD comprise a first-order kinetic model and a modified Gompertz model,
204 presented in equations (1) and (2) (Nguyen et al., 2019; Siripatana et al., 2016). Then
205 ultimate hydrogen or methane production and the hydrolysis constants are obtained
206 from the experimental data plot.

207

208 First–order kinetic model :$M(t) = M_m \times (1 - e^{-k \times t})$ (1)

209

210 Here *M(t)* is the cumulative production of hydrogen or methane at a given time (mL/g-
211 COD), M_m is the maximum cumulative production of hydrogen or methane (mL/g-
212 COD), *k* is the rate constant (1/h or 1/d), and *t* is the time (h or d).

213

214 Modified Gompertz model: $M(t) = M_m \times exp\left\{-exp\left[\frac{R_{max} \times e}{M_m}(\lambda - t) + 1\right]\right\}$ (2)

215

216 where R_{max} is the maximum specific of hydrogen or methane production rates (mL/g-
217 COD·h or mL/g-COD·d), λ is lag phase period or minimum time to produce biogas (h
218 or d), *t* is cumulative time for biogas production (h or d), and *e* is 2.718282, exp (1).
219 Microsoft Excel ™2010, with Solver add-in program (Microsoft, USA) was used to
220 determine the kinetic parameters .The correlation coefficients (R^2) were also obtained.

221

222 **3. Results and discussion**

223 3.1 Effect of RWA loading on biohydrogen and biomethane production

224 The cumulative H_2-TSAD of raw SLS and DSLS at various RWA loadings are

reported in Fig. 1a. No methane was detected during the hydrogen production in the first-stage AD. All DSLS gave higher hydrogen production than raw SLS. The highest 154.48 mL.H_2 cumulative hydrogen in the hydrogenic stage during 64 h of operation was achieved from DSLS5 (Fig. 1a), which corresponds to hydrogen yield of 90.64 mL-H_2/g-COD_{added}. A lower by a half cumulation of hydrogen at 75.48 mL-H_2 was obtained from raw SLS.

This obviously shows that, by using RWA, the sulfate in SLS could be reduced (data shown in Table 3) and this decreased the competition between hydrogen producing bacteria and sulfate reducing bacteria (SRB) for using the same organic matters as electron donors to reduce either hydrogen or hydrogen sulfide (Kongjan et al., 2014). Considering the RWA loading in SLS, 10 g/L RWA achieved the highest sulfate removal efficiency. The mechanism of RWA in sulfate removal from SLS is described in our previous work (Raketh et al., 2021). However, among the DSLS cases, DSLS5 provided the highest H_2 production, while sulfate content was higher than in DSLS10. Some metal ions can be leached from RWA and solubilized into SLS, as shown in Table 4 which were investigated by inductively coupled plasma optical emission spectrometry (ICP-OES) technique. The lower RWA loading should provide less metal ions, so that when the RWA loading increased the metal ion concentrations increased. Ni, Cu, and Mn slightly increase in DSLS while Mg was two times higher than in raw SLS. K was also increased in DSLS10 and higher than in raw SLS, exceeding the recommended level (2.5 mg/L) (Reungsang et al., 2019) and inhibiting the anaerobic system. Possibly in these concentration ranges the metal ion effects dominated over effects of the sulfate content.

DSLS is also a more promising substrate than raw SLS for methane production

both in CH_4-TSAD and CH_4-SSAD (Fig. 1b and Fig. 2). 50.02-75.95% methane contents in the biogas were observed, demonstrating favorable metabolic pathway (Reungsang et al., 2019; Raketh et al., 2021). Using DSLS gave 13-16% methane production increases from that of raw SLS. The highest methane productions of 502 mL-CH_4 and 520 mL-CH_4 were from DSLS10 in the CH_4-TSAD and the CH_4-SSAD processes, respectively. According to biomethane production protocols, the substrate in CH_4-TSAD and CH_4-SSAD assays was about 3-fold diluted by the inoculum. Thus, the concentrations of organic and inorganic compounds in SLS substrate were also reduced. This reduces the effects of RWA loading on CH_4-TSAD and CH_4-SSAD, compared to H_2-TSAD. DSLS10 achieved the highest methane productions in both CH_4-TSAD and CH_4-SSAD processes. This clearly demonstrates that at lower metal ion concentrations the sulfate content in DSLS significantly affected methane production.

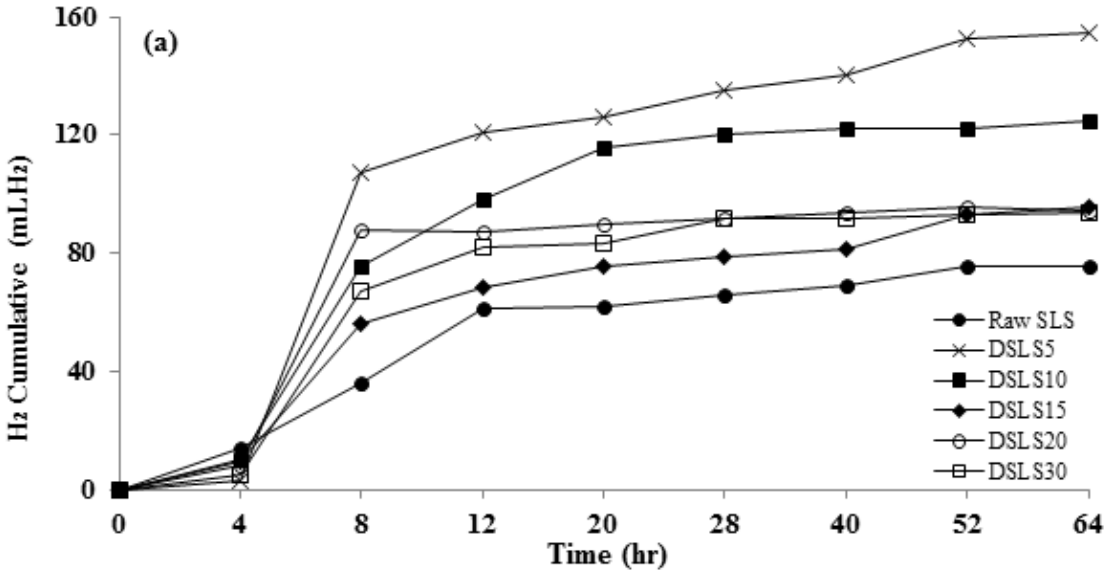

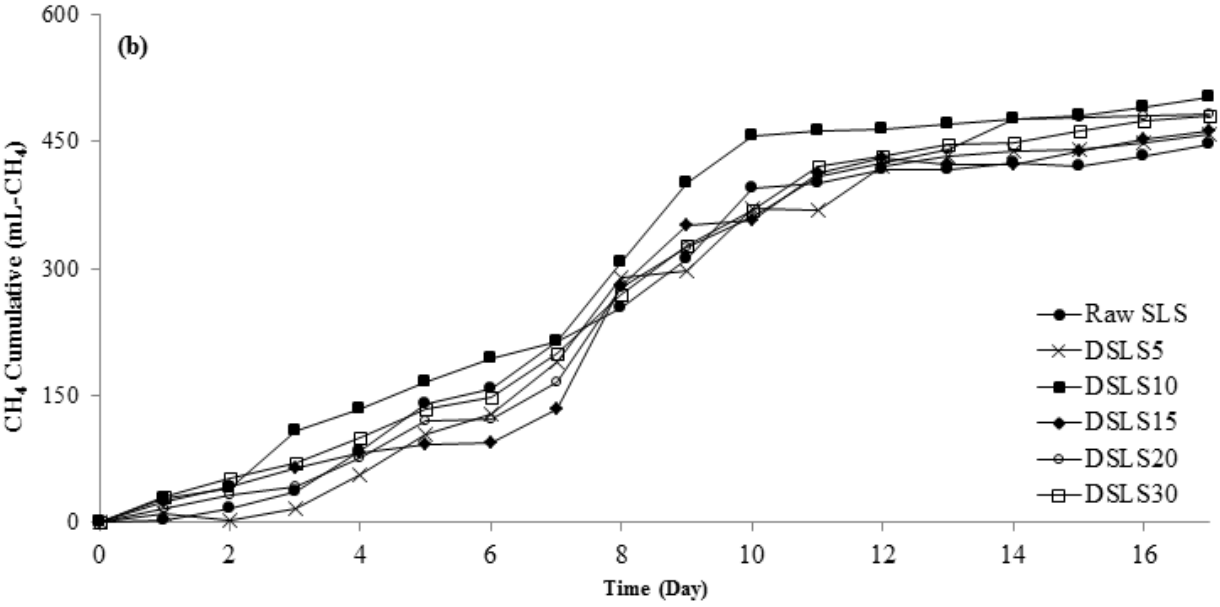

Fig.1 The experimental results from TSAD. (a) Cumulative hydrogen production, and (b) cumulative methane production.

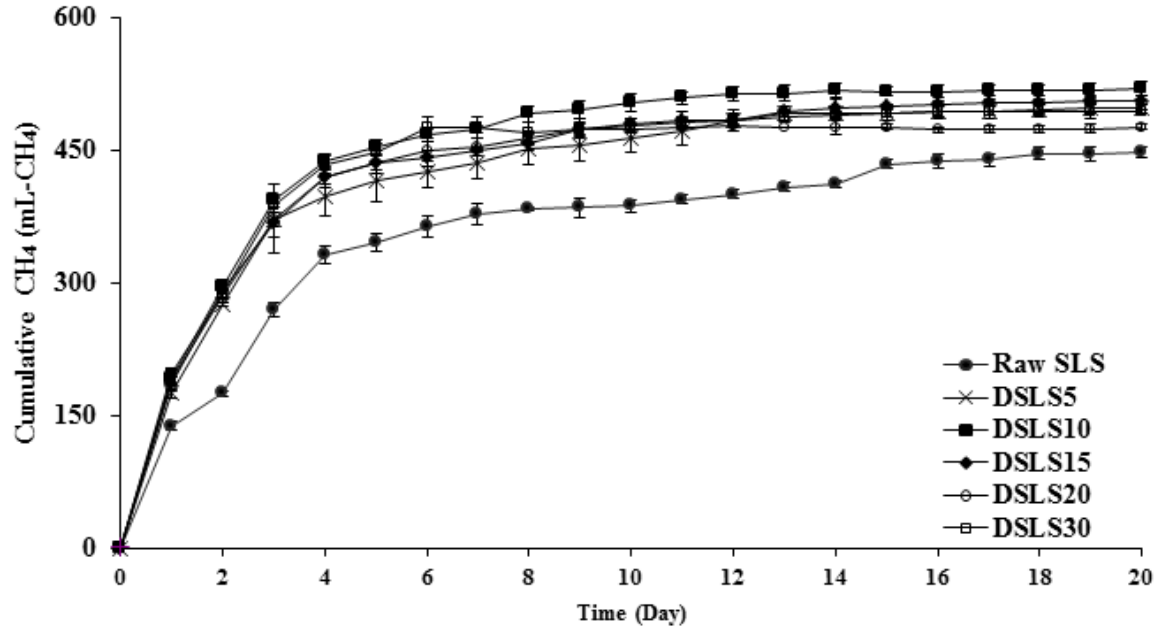

Fig.2 Cumulative methane production from SSAD

296 **Table 3** pH and sulfate concentration during H_2-TSAD, CH_4-TSAD, and CH_4-SSAD runs**.**

297

Substrate	Two-stage AD									Single-stage AD						
	H_2-TSAD			CH_4-TSAD			Sulfate mass distribution		Overall sulfate removal (%)	CH_4-SSAD				Sulfate mass distribution		Overall sulfate removal (%)
	Initial pH[a]	Final pH	Initial Sulfate (mg/L)	Initial pH	Final pH	Final Sulfate (mg/L)	Initial[b] (mg)	Final (mg)		Initial pH	Final pH	Initial Sulfate (mg/L)	Final Sulfate (mg/L)	Initial[c] (mg)	Final (mg)	
Raw SLS	7.00	6.93	5417	7.56	7.64	261	325	52	83.94	7.31	7.34	1625	250	325	50	84.62
DSLS5	7.03	6.94	3467	7.6	7.65	155	208	31	85.10	7.49	7.33	1040	145	208	29	86.11
DSLS10	6.98	6.86	2833	7.55	7.63	111	170	22	86.94	7.58	7.35	850	102	170	20	88.00
DSLS15	7.00	6.93	3267	7.61	7.65	149	196	30	84.80	7.6	7.34	980	145	196	29	85.20
DSLS20	7.06	6.95	4100	7.62	7.66	152	246	30	87.64	7.65	7.37	1230	149	246	30	87.89
DSLS30	7.12	6.98	4333	7.63	7.66	174	260	35	86.62	7.68	7.4	1300	170	260	34	86.92

[a] pH adjusted with $NaHCO_3$, [b] Working volume of H_2-TSAD was 60 mL, and [c] Working volume of CH_4-SSAD was 120 mL

298

299

300

301

302

303

304

Table 4 Dissolved elements in raw SLS and DSLS10 from ICP-OES technique.

Dissolved element	Concentration (mg/L)	
	Raw SLS	DSLS10
Cobalt (Co)	< 0.003	< 0.003
Nickel (Ni)	< 0.005	0.06±0.01
Copper (Cu)	< 0.016	0.18 ± 0.02
Manganese (Mn)	0.14 ± 0.00	2.69 ± 0.00
Iron (Fe)	0.60 ± 0.02	1.34 ± 0.02
Sodium (Na)	10.62 ± 0.02	12.22 ± 0.09
Calcium (Ca)	12.91 ± 0.05	302.40 ± 6.56
Magnesium (Mg)	32.41 ± 0.06	66.41 ± 0.10
Phosphorus (P)	223.90 ± 2.64	209.20 ± 1.56
Zinc (Zn)	295.70 ± 3.93	240.80 ± 2.88
Potassium (K)	3,728.00 ± 47.85	4,015.00 ± 59.26

Under anaerobic conditions, sulfate reducing bacteria (SRB) use sulfate as a terminal electron acceptor to suppress organic compounds (Mu et al., 2019). The SRB is not only competing with methane-producing bacteria (MPB) to use organic substances resulting in lower methane production yield (Gustavsson et al., 2013), but SRB also could produce a significant amount of H_2S from sulfate in SLS, which inhibits MPB, causing slowing or stop of the methane production. Fig. 3 shows the cumulative H_2S from TSAD and SSAD processes. As expected, the more sulfate was in the substrate, the more H_2S was produced. In both TSAD and SSAD processes, the raw SLS digestion produced the most H_2S by cumulative volume and its concentration in biogas ranged within 0.21-3.57%. The lowest cumulative H_2S was given by DSLS10 digestion and the concentration in biogas ranged within 0.22-1.56%. The TSAD started to generate H_2S on the 2^{nd} day of fermentation (Fig. 3a), whereas H_2S was detected after the 3^{rd} day from SSAD, as illustrated in Fig. 3b. This is because sulfates are consumed in the first

stage and converted to hydrogen sulfide. Organic substrates in H_2-TSAD are also utilized by SRB and produce HS^-. Thus, the effluent of H_2-TSAD, which was the feed to CH_4-TSAD, was rich in SRB and HS^- causing H_2S detection early on from this stage. In contrast, SRB in SSAD took the time for favorable growth in the methane production processes, hence H_2S was generated later than by TSAD. This investigation found that the TSAD produced 6% less cumulation of H_2S than the SSAD process.

RWA does not reduce the sulfate to lower than the inhibition level (500 mg/L) due to the equilibrium limit and because sulfate contained in RWA was released into SLS (Raketh et al., 2021). However, RWA clearly enhanced the biogas production from DSLS which was higher than from raw SLS both in TSAD and SSAD processes. Sulfate concentrations and sulfate mass distribution during H_2-TSAD, CH_4-TSAD, and CH_4-SSAD runs were also observed and are shown in Table 3. It was found that the overall sulfate removal efficiencies (83.94-88.00%) achieved were similar for TSAD and SSAD processes in SLS digestion.

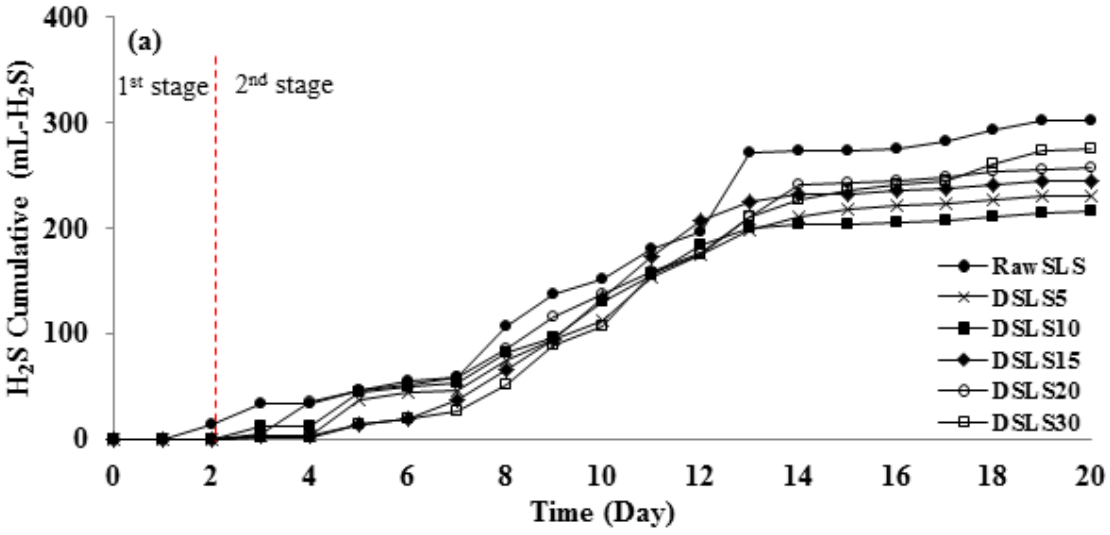

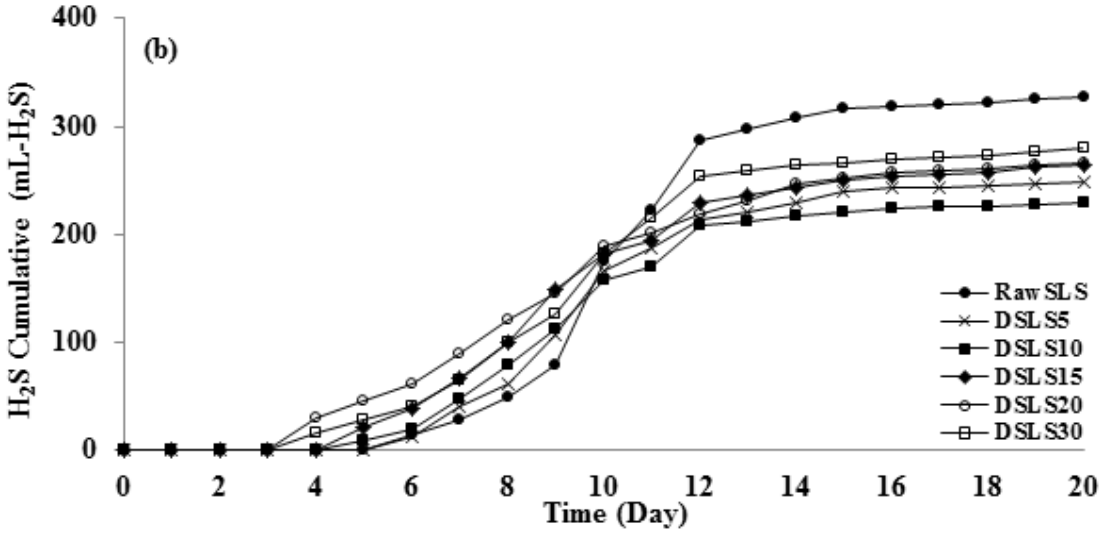

Fig. 3 Cumulative hydrogen sulfide production from (a) TSAD, and (b) SSAD.

3.2 Kinetics study

H_2 and CH_4 production rates are also important for further process design, so it is necessary to simplify and accurately explain the mechanisms and metabolic pathways related to AD of the substrates under varied operating conditions, for predicting the performance of an individual digester (Nguyen et al., 2019). The kinetic parameters of the models used to explain the rates of substrate degradation and H_2-TSAD, CH_4-TSAD, and CH_4-SSAD were determined by model fits to the experimental data. Table 5 summarizes the results of kinetic study of TSAD and SSAD processes using the first-order kinetic model and the modified Gompertz model.

Using the first-order kinetic model, H_2-TSAD ($R^2 > 0.91$), and CH_4-SSAD ($R^2 > 0.96$) data were fitted better than the CH_4-TSAD data ($R^2 > 0.90$). This is probably due to high VFAs in substrate loaded into CH_4-TSAD, which could slow down the methanogen activity. Moreover, the first-order kinetic model provided higher R^2 than 0.90 and was appropriate in all these cases. This is reconfirmed by plots of measured

and model predicted H_2-TSAD, CH_4-TSAD, and CH_4-SSAD in Fig. 4. The predicted H_2-TSAD by the model was slightly below the experimental results. For CH_4-TSAD, both of models slightly overestimated the experiments, in contrast to the CH_4-SSAD for which model predictions were below the values from experiments. The rate constants (*k*) of first-order models varied in the range 0.12-0.31 (1/h) for H_2-TSAD and 0.11-0.51 (1/d) for CH_4-TSAD and CH_4-SSAD.

Theoretically, methane production rate in CH_4-TSAD should faster than in CH_4-SSAD because some organic matter, especially carbohydrates, is degraded during the first stage before feeding to the second. It can be observed that most studies reporting faster methane production rate in the CH_4-TSAD used difficult to digest substrates. Sani et al. (2021) report on biohydrogen and biomethane potential of palm oil mill effluent (POME). The POME is a poorly digestible substrate, and the *k* for CH_4-TSAD (0.12-0.39) is higher than for CH_4-SSAD (0.08-0.27) (Sani et al., 2021). On the other hand, in this study the *k* of first-order kinetic model for CH_4-SSAD (0.24-0.51) was higher than for CH_4-TSAD (0.11-0.14) as shown in Table 5.

For the modified Gompertz model, different interpretable parameters of M_m, R_{max}, and λ were obtained by fitting with cumulative production of hydrogen and methane (Fig.4). The R^2 values were in range 0.92-0.99 of H_2-TSAD, 0.96-0.99 of CH_4-TSAD, and 0.94-0.9789 of CH_4-SSAD. The R^2 of the modified Gompertz model fits was excellent indicating good suitability of this model type, and good correlation to experimental data to explain cumulative production of hydrogen and methane from AD process. λ of H_2-TSAD and CH_4-SSAD were shorter than for CH_4-TSAD, indicating microorganisms in an inoculum used are rapidly starting AD of the substrate. The lag time of raw SLS of H_2-TSAD was shorter than of DSLS, while in contrast DSLS10 of

both CH_4-TSAD and CH_4-SSAD achieved a shorter lag time than others. Therefore, the RWA loading affects lag time. Nonetheless, the modified Gompertz model is not directly related to biogas or other kinds of accumulated product data in a context of enzymatic kinetics (Siripatana et al., 2016), hence using kinetic constant obtained from the first-order kinetic model in combination with those interpretable parameters attained from the modified Gompertz model could be further used, possibly for optimizing the design, start-up, and functioning of a continuous anaerobic digester.

Table 5 Kinetic parameters according to model fits for TSAD and SSAD processes.

	H_2-TSAD						CH_4-TSAD						CH_4-SSAD					
	rawSLS	DSLS5	DSLS10	DSLS15	DSLS20	DSLS30	rawSLS	DSLS5	DSLS10	DSLS15	DSLS20	DSLS30	rawSLS	DSLS5	DSLS10	DSLS15	DSLS20	DSLS30
Experimental M_m (mL/g-COD)	44.29	90.64	73.04	56.02	56.16	55.11	261.68	269.35	294.53	271.48	283.38	281.62	263.28	292.77	305.10	297.17	279.86	290.42
First order model																		
M_m (mL/g-COD)	41.54	79.44	67.69	46.42	52.26	48.22	281.24	270.06	305.80	293.96	293.45	296.86	263.74	290.93	301.34	293.57	278.63	288.06
k^*	0.12	0.19	0.17	0.21	0.26	0.31	0.12	0.13	0.14	0.11	0.12	0.12	0.24	0.35	0.45	0.39	0.51	0.49
R-Squared	0.9514	0.9343	0.9927	0.9442	0.9169	0.9887	0.9571	0.9352	0.9373	0.9002	0.9296	0.9402	0.9626	0.9793	0.9913	0.9855	0.9956	0.9892
Modified Gompertz model																		
M_m (mL/g-COD)	44.13	88.00	73.00	50.09	54.64	53.25	271.66	263.32	316.97	279.61	307.83	309.32	243.04	278.12	296.49	283.83	274.92	283.32
Lag time**	1.01	3.98	2.50	1.95	2.89	2.85	2.60	2.69	1.93	3.15	3.20	2.25	0.63	0.43	0.15	0.39	0.51	0.55
R_{max}***	3.28	15.02	8.39	4.93	11.21	7.63	31.01	33.01	32.34	35.92	32.39	28.44	66.37	97.86	93.77	101.36	114.56	119.80
R-Squared	0.9248	0.9591	0.9908	0.9372	0.9818	0.9766	0.9904	0.9908	0.9784	0.9616	0.9902	0.9891	0.9404	0.9470	0.9768	0.9556	0.9629	0.9602

* k in (1/h) for H_2-TSAD; and k in (1/d) for CH_4-TSAD and CH_4-SSAD.

** Lag time in (h) for H_2-TSAD; and in (d) for CH_4-TSAD and CH_4-SSAD.

*** R_{max} in (mL/g-COD-h) for H_2-TSAD; and in (mL/g-COD-d) for CH_4-TSAD and CH_4-SSAD.

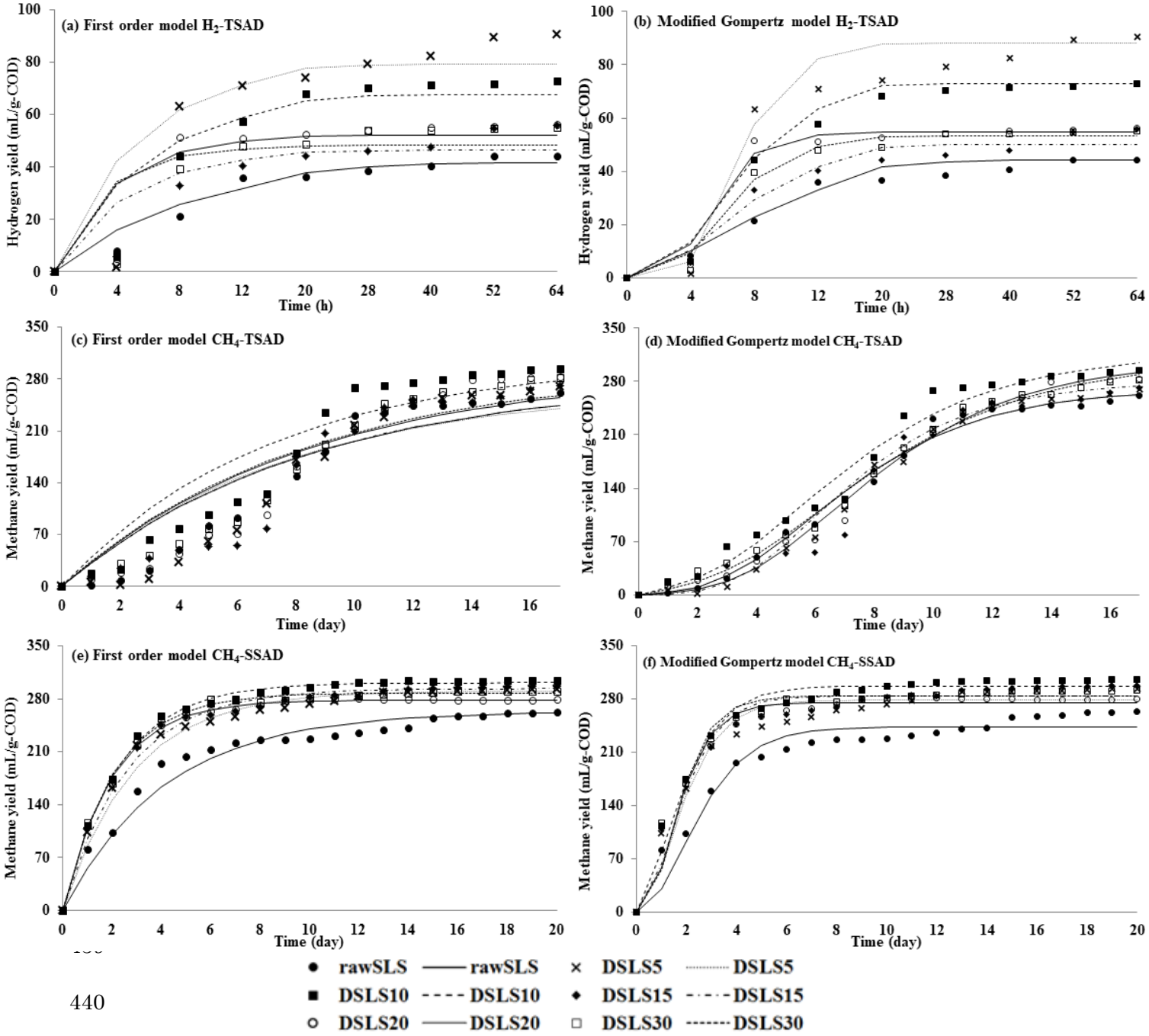

Fig. 4 Experimental data (symbols) and model fits (lines) of cumulative production yield from TSAD and SSAD process: (a) First order model of H_2-TSAD, (b) Modified Gompertz model of H_2-TSAD, (c) First order model of CH_4-TSAD, (d) Modified Gompertz model of CH_4-TSAD, (e) First order model of CH_4-SSAD, and (f) Modified Gompertz model of CH_4-SSAD.

448 Table 6 shows VFA (acetic, propionic, and butyric acid) profiles of all
449 experiments. Rich VFAs of 1.32-2.90 g/L acetic, 2.05-3.47 g/L propionic, and 6.21-7.60
450 g/L butyric acid were observed from H_2-TSAD. Wang et al. (2009) reported the
451 optimum conditions for acetic acid, propionic acid, and butyric acid at concentrations of
452 1.6, 0.3, and 1.8 g/L, respectively, as those giving the maximum cumulative methane
453 yield. Nevertheless, the inhibiting levels of VFAs are 2.0 g/L of acetic acid (Demirel
454 and Yenigün, 2002), 0.9 g/L of propionic acid (Wang et al., 2009) and, 4.5 g/L of butyric
455 acid (Aguilar et al., 1995). SLS has a high carbohydrate content in the form of
456 fermentable sugar. Danwanichakul et al. (2019) reported that SLS contained 1.2 g/L L-
457 Quebrachitol. Thus, the sugar can be mostly consumed during acidogenesis step and this
458 produces high VFAs. It can be seen from Table 6 that initially CH_4-TSAD contained
459 propionic acid at a concentration near the inhibition level, and contained VFAs at a
460 higher level than CH_4-SSAD. This made CH_4-TSAD give a lesser CH_4 production in the
461 first period. Even though the microorganisms in CH_4-TSAD needed more time for
462 acclimation, the final methane yield achieved was similar to CH_4-SSAD.
463 Feng et al., 2017 and Lyberatos and Pullammanappallil, 2010 present reactions
464 that can take place in hydrogen production. The pathways of acetic and butyric
465 production shown in equations (3) and (4) are the main pathways of hydrogen
466 production during acidogenesis stage. The stoichiometrically calculated H_2 production
467 yields based on equations (3) and (4) are compared to the experimental yields in Table
468 7. It was found that the experimental H_2 production yields are lower than the calculated
469 theoretical H_2 production yields in all AD process cases. This can be explained by other
470 pathways generating acetate, propionate, and butyrate but without hydrogen production,
471 as shown in equations (5) and (6). Moreover, propionate producing during AD process

is probably generated via the pathway showing in equations (7) which the produced H_2 and sugar are consumed. (Feng et al., 2017; Lyberatos and Pullammanappallil, 2010; Sani et al., 2021).

$$C_6H_{12}O_6 + 2H_2O \longrightarrow 2CH_3COOH + 2CO_2 + 4H_2 \quad (3)$$

$$C_6H_{12}O_6 + 2H_2O \longrightarrow CH_3CH_2CH_2COOH + 2CO_2 + 2H_2 \quad (4)$$

$$3C_6H_{12}O_6 \longrightarrow 4CH_3CH_2COOH + 2CH_3COOH + 2CO_2 + 2H_2O \quad (5)$$

$$4C_6H_{12}O_6 + 2H_2O \longrightarrow 2CH_3COOH + 3CH_3CH_2CH_2COOH + 8CO_2 + 10H_2O \quad (6)$$

$$C_6H_{12}O_6 + 2H_2 \longrightarrow 2CH_3CH_2COOH + 2H_2O \quad (7)$$

The optimum pH in acidogenesis and methanogenesis stages is 5-6.7 and 7-8, respectively (Kongjan et al., 2018). In H_2-TSAD, pH slightly dropped due to the addition of $NaHCO_3$ to maintain the pH and buffer capacity of the system at their initial levels. All of the cases H_2-TSAD, CH_4-TSAD and CH_4-SSAD had a suitable initial pH in the ranges 6.98-7.12 and 7.31-7.68, respectively, as presented in Table 3.

Table 6 Volatile fatty acids on TSAD and SSAD**.**

Sample	H_2-TSAD						CH_4-TSAD			CH_4-SSAD		
	Initial (g/L)			Final (g/L)			Initial (g/L)			Initial (g/L)		
	Acetic	Propionic	Butyric	Acetic	Propionic	Butyric	Acetic	Propionic	Butyric	Acetic	Propionic	Butyric
Raw SLS	0.88	0.81	0.62	1.32	2.05	6.94	0.40	0.62	2.08	0.26	0.24	0.19
DSLS5	0.91	0.83	0.64	2.90	3.47	7.25	0.87	1.04	2.18	0.27	0.25	0.19
DSLS10	0.92	0.81	0.66	2.34	2.79	7.60	0.70	0.84	2.28	0.28	0.24	0.20
DSLS15	0.96	0.85	0.69	1.79	2.38	6.72	0.54	0.71	2.02	0.29	0.26	0.21
DSLS20	1.01	0.89	0.73	1.77	2.35	6.21	0.53	0.71	1.86	0.30	0.27	0.22
DSLS30	1.06	0.94	0.76	1.76	2.34	6.17	0.53	0.70	1.85	0.32	0.28	0.23

505 **Table 7** Stoichiometric calculation of H_2 generation yield from produced VFAs.

506

Substrate	VFAs appeared in H_2-TSAD				Stoichiometrically calculated H_2 production					Experimental H_2 production
	Acetic		Butyric		H_2 from acetic		H_2 from butyric		Total H_2	Total H_2
	(g/L)	(mmol)[a]	(g/L)	(mmol)[a]	(mmol)	mL(STP)	(mmol)	mL(STP)	mL (at 55°C)	mL (at 55°C)
Raw SLS	0.44	0.44	6.32	4.31	0.88	19.71	8.62	193.05	255.62	75.48
DSLS5	1.99	1.99	6.61	4.51	3.99	89.30	9.01	201.91	349.87	154.48
DSLS10	1.42	1.42	6.94	4.73	2.84	63.62	9.46	211.99	331.13	124.48
DSLS15	0.83	0.83	6.03	4.11	1.66	37.18	8.22	184.09	265.85	95.48
DSLS20	0.76	0.76	5.48	3.74	1.53	34.20	7.48	167.49	242.32	95.77
DSLS30	0.70	0.70	5.41	3.69	1.40	31.36	7.38	165.25	236.22	93.93

[a] using working volume = 0.06 L for H_2-TSAD

507

508

509

510

511

512

513 3.3Anaerobic biodegradability

514 After 14 days of the CH_4-TSAD and 12 days of the CH_4-SSAD runs, a nearly
515 steady methane production rate was observed. The overall COD distributions for the
516 TSAD and SSAD processes are presented in Table 8. It was found that both systems
517 gave an overall COD removal efficiency exceeding 65 % and the difference between the
518 two systems was not significant, although % COD removal efficiency of the TSAD was
519 slightly higher.

520 In TSAD, the highest COD removal efficiency of 78.02 % was achieved with
521 DSLS10 while raw SLS gave the lowest COD removal efficiency of 68.10%. In the
522 SSAD process, more than 70 % of COD removal was attained in DSLS digestion.
523 DSLS10 gave the maximum COD removal (76.37%), whereas 65.90 % COD removal
524 was attained with raw SLS.

525 An enhancement in the COD removal efficiency from using DSLS demonstrates
526 that the substrate was more suited to the microorganisms metabolizing it than raw SLS
527 was. DSLS had a lower initial sulfate concentration than raw SLS, resulting in less
528 competition of SRB and MPB, and MPB can digest the organic compounds in DSLS
529 better than in raw SLS, in the lower H_2S environment.

530

531 **Table 8** COD balance for the TSAD and the SSAD processes.

Sample	COD converted to gaseous compound (g)		COD in liquid phase (g)		Overall COD removal (%)
	H_2 production	CH_4 production	Initial [a]	Final [b]	
	Two stages AD				
Raw SLS	0.04	1.13	1.72	0.55	68.10
DSLS5	0.09	1.16	1.72	0.47	72.75
DSLS10	0.07	1.27	1.72	0.38	78.02

DSLS15	0.06	1.17	1.72	0.50	71.25
DSLS20	0.06	1.22	1.72	0.45	74.19
DSLS30	0.06	1.22	1.72	0.45	73.73
Single stage AD					
Raw SLS	-	1.14	1.72	0.59	65.90
DSLS5	-	1.26	1.72	0.46	73.28
DSLS10	-	1.32	1.72	0.41	76.37
DSLS15	-	1.28	1.72	0.44	74.38
DSLS20	-	1.21	1.72	0.52	70.05
DSLS30	-	1.25	1.72	0.47	72.70

[a] COD in substrate.
[b] Remaining COD in fermentation broth was calculated from COD balance.

3.4 Hydrogen and methane energy yields

Hydrogen and methane production yields together with overall energy production yields from each substrate in TSAD and SSAD processes were calculated and are shown in Table 9. For the TSAD, energy production in H_2-TSAD ranged in 0.47-0.97 kJ/g-COD_{added} and the DSLS5 fermentation gave the highest 90.64 mL-H_2/g-COD_{added} yield (0.97 kJ/g-COD_{added}), which is 16.15% of the theoretical yield (467 mL-H_2/g-COD_{added}).

A low substrate conversion was obtained in the first stage because only short chain carbohydrates were digested (Liu et al., 2013). The comparatively low hydrogen yields of raw SLS relative to DSLS were due to the higher sulfate content in raw SLS.

The CH_4-TSAD generated energy in the range 8.30-9.35 kJ/g-COD_{added}. The maximum yield was from DSLS10 at 294.53 mL-CH_4/g-COD_{added} (9.35 kJ/g-COD_{added}) which is 74.59% of the theoretical yield (350 mL-CH_4/g-COD_{added}). The SSAD process produced more methane corresponding to energy range 8.35-9.68 kJ/g-COD_{added}, and the DSLS10 gave the highest yield of 305.09 mL-CH_4/g-COD_{added} (9.68 kJ/g-COD_{added}), which is 77.26 % of the theoretical yield. The lower yield of methane from TSAD was

because some COD was converted to H_2 in the first stage of AD. However, when the overall energy production was assessed, it was 5% higher for TSAD than for SSAD process.

Table 9 Summary of hydrogen and methane yields from TSAD and SSAD processes.

		Hydrogen production		Methane production		Overall energy production yield (kJ/g-COD_{added})		
		Yield (mL/g-COD_{added})	% of theoretical Yield*	Yield (mL/g-COD_{added})	% of theoretical Yield*	H_2	CH_4	Total
Two-stage AD	Raw SLS	44.29	7.89	261.68	66.27	0.47	8.30	8.78
	DSLS5	90.64	16.15	269.35	68.21	0.97	8.55	9.51
	DSLS10	73.03	13.02	294.53	74.59	0.78	9.35	10.12
	DSLS15	56.02	9.98	271.48	68.75	0.60	8.61	9.21
	DSLS20	55.43	9.88	283.38	71.77	0.59	8.99	9.58
	DSLS30	55.11	9.82	281.62	71.32	0.59	8.94	9.52
Single-stage AD	Raw SLS	-	-	263.28	66.68	-	8.35	8.35
	DSLS5	-	-	292.77	74.14	-	9.29	9.29
	DSLS10	-	-	305.09	77.26	-	9.68	9.68
	DSLS15	-	-	297.17	75.26	-	9.43	9.43
	DSLS20	-	-	279.86	70.87	-	8.88	8.88
	DSLS30	-	-	290.42	73.55	-	9.22	9.22

* H_2 and CH_4 theoretical yields of 467 mL/g-COD glucose at STP and 350 mL/g-COD at STP.

In most cases the TSAD was more productive than the SSAD process, because TSAD offers several advantages. The TSAD is split in stages that allow separately optimizing hydrolysis/acidogenesis and methanogenesis, to improve the overall reaction rate, maximize biogas yields, and make the process easier to control, both in meso- and thermophilic states. In addition, TSAD is enriching different microorganisms in each anaerobic digester (Schievano et al., 2012). Similarly, better process conversion efficiency and maximum overall energy yield were reported previously for TSAD, it

being more productive than SSAD.

Table 10 has a comparison of TSAD and SSAD process performances on using several substrates, in the form of total energy recovery. Sani et al. (2021) reported a comparative evaluation of SSAD and TSAD using palm oil mill effluent. The results showes a 38.95% higher total energy production for TSAD compared to SSAD. Similar results were reported by Massanet-Nicolau et al. (2013) and Akobi et al. (2016), who observed over 30% increases in overall energy recovery for TSAD compared to SSAD, with wheat pellet and poplar wood substrates, respectively. Arreola-Vargas et al. (2016) reported similarly a 22% increase when bagasse was used as the substrate. Moreover, food waste was also used as the substrate in an investigation of overall energy recovery, and De Gioannis et al. (2017) and Nathao et al. (2013) reported 20 and 18 % higher energy recoveries for TSAD.

Aside from that, there is a case that reported no significant differences in overall energy recovery for TSAD and SSAD systems using a mixture of swine manure and market biowaste as the substrate (Schievano et al., 2012). This suggests the hypothesis that TSAD may in some cases have no advantage in terms of the overall energy recovery. This is somewhat conflicting with various prior studies. The listing in Table 10 was arranged starting from more difficult to digest substrates. Therefore, it is in a good agreement with our study, in which DSLS is easier to biodegrade compared to the other substrates, and only a 5% increase in overall energy recovery was obtained. Thus, the total energy recovery depends strongly on both substrate and operating conditions. The various substrates gave different total energy recoveries, as mentioned above, and different operating conditions also affected energy recovery.

586 **Table 10** Total energy recovery in forms of hydrogen and methane production by TSAD

587 and by SSAD processes.

Substrate	Total Energy Recovery		% increase	Reference
	Single-stage	Two-stage		
Palm oil mill effluent	9.79 kJ/gCOD$_{feedstock}$	13.61 kJ/gCOD$_{feedstock}$	38.95	(Sani et al., 2021)
Wheat feed pellets	8.73 MJ/kg-VS	12.09 MJ/kg-VS	37	(Massanet-Nicolau et al., 2013)
Poplar wood	8.70 kJ/gCOD$_{feedstock}$	11.60 kJ/gCOD$_{feedstock}$	33	(Akobi et al., 2016)
Bagasse	12.80 kJ/L	35.80 kJ/L	22	(Arreola-Vargas et al., 2016)
Food waste	11.60 MJ/kg-VS	14.50 MJ/kg-VS	20	(De Gioannis et al., 2017)
Food waste	3.40 × 10^{-3} kW-h	4.00 × 10^{-3} kW-h	18	(Nathao et al., 2013)
Mixture of swine manure and market biowaste	14.21 kJ/kg-VS$_{added}$	14.13 kJ/kg-VS$_{added}$	No sd*	(Schievano et al., 2012)
DSLS10	9.68 kJ/g-COD$_{added}$	10.12 kJ/g-COD$_{added}$	5	This study

*No sd means "not significant difference"

588

589 3.5 Cost assessment and energy outcome from AD process

590

591 The costs assessment with DSLS10 substrate for SSAD and TSAD was based on

592 400 m^3/d wastewater production of the concentrated latex factory in Songkhla province,

593 Thailand. Continuous stirred tank reactors (CSTR) were chosen for both SSAD and

594 TSAD processing of DSLS10. Firstly, Organic loading rate (OLR) (g-COD/L·d) was

595 calculated from equation (8) (Kongjan et al., 2018)

596

597 $$OLR = \frac{kC_o}{y/(y_m - y)} \quad (8)$$

598

599 Here C_0 is the initial concentration of substrate equaling 8 g-COD /L, y is the

600 required hydrogen/methane yield (mL/g-COD$_{added}$), and y_m is the ultimate

hydrogen/methane yield at the end of hydrogen/methane production assay (mL/g-COD_{added}). Then the working volume of CSTR (V_R) can be calculated from equation (9)

$$V_R = Q \cdot C_0 / OLR \quad (9)$$

Here, Q is influent flow rate (m^3/d). The purchase cost, variable cost, and revenues were calculated and are summarized in Table 11. The total purchase cost will vary depending on the type of reactor and its size, and the mixing system. The results show that the purchase cost of TSAD is higher than of SSAD, and these are estimated as 707,172 and 1,131,693 USD, respectively. TSAD needs more investment because it includes 2 digesters for H_2-TSAD and CH_4-TSAD, has a lower digestion rate, and operates at the higher temperature of 55ºC. There are very few studies that report a comparison of purchase costs between SSAD and TSAD. 46% higher purchase cost of SSAD required for DSLS in this study is much higher than the 3% more expensive SSAD for food waste reported by Rajendran et al. (2020).

The variable costs consisted of labor, operating costs (electricity cost for pumping and digester, upgrading costs, and power generation costs), and maintanance costs. The total variable costs of TSAD were 239,145 USD/year while for SSAD they were 177,397 USD/year. The revenues were calculated from the electricity produced from the purified biogas. The revenue of gas from TSAD was comparatively higher than that from SSAD by 9%, due to the higher energy yield described in a previous section.

The payback time was evaluated for purchase cost using the profit difference of revenues and variable costs. Even though the revenue was higher for TSAD than for

SSAD, TSAD had a larger investment, so its payback time at 4.36 years was longer than for SSAD at 2.52 years.

There is a lack of reports on payback time of electricity production from biogas generated from TSAD, while some reports on SSAD are accessible. Chungchaichana and Vivanpatarakij (2012) reported a 3 years payback time for 94.19 ton/day fresh-food market waste treatment for biogas production (17,807 m^3/day) used to produce electricity (12,643 - 24,929 kWh). An AD plant for animal manure, built and operated by Ilci Agricultural, Livestock & Biogas Company in Turkey, has a reasonable energy based payback time of 3.7 years when using the SSAD process (Akbulut, 2012). In addition, the mature technology that uses dairy cattle manure and corn insilate co-digestion to produce biogas and convert it to electricity via Solid Oxide fuel cells, has the reasonable 4 years payback time for large-sized plants (manure availability 103.5 tons/day) (Baldinelli et al., 2018).

As a practical assessment, the advantages of TSAD include providing optimum operating conditions by stage separation, faster degradation of substrates, and higher loading. On the other hand, the disadvantages include ammonia accumulation due to recirculation that might be toxic to the microbes, uncertainty around reactor configuration for several feedstock types, and poor economic viability (Rajendran et al., 2020). Therefore, the disadvantages of the TSAD need considerable research. The calculations indicate that TSAD is not economically attractive for DSLS10. Hence, there is low potential for replacing SSAD with TSAD in treatment of DSLS10. However, studies on continuous AD production in pilot-scale with variations of OLRs are required for evaluating the real kinetic parameters needed in digester sizing.

Category	SSAD	TSAD	Units	References

Table 11 Cost assessment and energy outcomes for SSAD and TSAD processes.

Design parameter				
Wastewater production (8 g-COD/L)	400	400	m^3/d	Based on Top Glove Technology factory data
OLR (Estimate from equation (3)) [a]	0.60	0.60 and 0.39	g-COD/L·d	(Kongjan et al., 2018)
HRT	13	0.56 and 21	d	(Kongjan et al., 2018)
Size of CSTR reactor (Estimate from equation (4))	5,910	245 and 9,026	m^3	(Rajendran et al., 2020)
Investment costs				
Digester				
CSTR reactor (assumed based on literature)	704,822	1,111,993	USD	(Rajendran et al., 2020; Vo et al., 2018)
Mixer pump [b] (4kW)	1,000	2,000	USD	(Alibaba., 2021)
Total facility investment				
Pump Power:2 pumps in each stage [c] (1.5 kW)	1,350	2,700	USD	(Kreng thai wattana., 2021)
Heat Exchanger	-	15,000	USD	(Han et al., 2016)
Total	**707,172**	**1,131,693**	**USD**	
Variable costs				
Labor wages (gross)				
2 operators in each AD process	7,091	7,091	USD/year	(Vo et al., 2018)
Operating				
Electricity cost of pump power and digester [d]	8,640	17,512	USD/year	
Upgrading cost [e]	118,732	151,300	USD/year	(Patterson et al., 2011)
Power generation cost [f]	16,770	21,370	USD/year	(Department of alternative energy development and efficiency., 2013)
Maintenance costs				
3% equipment purchase cost	21,215	33,951	USD/year	(Vo et al., 2018)
0.7% insurance	4,950	7,922	USD/year	(Vo et al., 2018)
Total	**177,397**	**239,145**	**USD/year**	
Revenues				
Cumulative biogas production [g]	670,802	854,801	m^3-biogas/year	This study
Electricity production [h]	1,992,282	2,167,786	kWh/year	(Abdelsalam et al., 2019)
Revenues from gas [i]	**458,225**	**498,591**	**USD/year**	(Kavitha et al., 2015)
Payback time	**2.52**	**4.36**	**year**	(Sritrakul, 1995)

[a] k constant was chosen from first order kinetic model for calculation OLRs, [b] QJB Series, QJB4/12-620/3-480/S, [c] EBARA, DVSA Series, 80DVS 51.5, [d] 0.18USD/kWh, [e] 0.18 USD/m^3-biogas (water scrubbing method), [f] 0.025 USD/m^3-biogas, [g] 85% of maximum yield in this study, [h] energy conversion efficiency 45% ; energy content 6.60 kWh/m^3-produced gas (SSAD); 1.15 kWh/m^3-produced gas (H_2-TSAD); 6.80 kWh/m^3-produced gas (CH_4-TSAD), and [i] estimation of output from energy was obtained from 1 kWh = 0.23USD.

4. Conclusions

This study indicated that RWA can reduce sulfate content in SLS and thereby improve biogas production and biogas quality from both TSAD and SSAD processes. The methane yields in second stage of TSAD and SSAD were found not significantly different. However, hydrogen was also collected in the first stage of TSAD, so that the total energy recovery from TSAD (in forms of H_2 and CH_4) was improved by 5% compared with the SSAD process. Furthermore, the cost assessment of continuous AD process was based on kinetics and yields in batch experiments, and it suggested that the payback time of TSAD (4.36 years) is longer than that of SSAD (2.52 years), because methane production in the second stage of TSAD is slower than in SSAD so that a larger digester is needed. Based on information from batch experiments, there is low potential for replacing SSAD with TSAD to treat DSLS10, according to this cost assessment. Further work is necessary to study continuous AD production on a pilot-scale, with variation of OLRs, to investigate the kinetic parameters further for digester sizing.

Acknowledgements

This research was financially supported by the Thailand Research Fund through the Royal Golden Jubilee Ph.D. Program (Grant No. PHD/0216/2559). The authors would like to thank the concentrated latex factory and the glove factory in Songkhla Province, Thailand for providing materials to our research. The fifth author is supported by the Thailand Research Fund under Grant No. RTA 6280014. In addition, the authors are also grateful to Assoc. Prof .Seppo Karrila, Prince of Songkla University, Surat

Thani campus, for proofreading a manuscript draft.

References

Abdelsalam, E.M., Samer, M., Attia, Y.A., Abdel-Hadi, M.A., Hassan, H.E., Badr, Y., 2019. Effects of Laser Irradiation and Ni Nanoparticles on Biogas Production from Anaerobic Digestion of Slurry. Waste and Biomass Valorization 10, 3251–3262. https://doi.org/10.1007/s12649-018-0374-y

Aguilar, A., Casas, C., Lema, J.M., 1995. Degradation of volatile fatty acids by differently enriched methanogenic cultures: kinetics and inhibition. Water Res. 29, 505–509. https://doi.org/10.1016/0043-1354(94)00179-B

Akbulut, A., 2012. Techno-economic analysis of electricity and heat generation from farm-scale biogas plant: Çiçekdağı{dotless} case study. Energy 44, 381–390. https://doi.org/10.1016/j.energy.2012.06.017

Akobi, C., Yeo, H., Hafez, H., Nakhla, G., 2016. Single-stage and two-stage anaerobic digestion of extruded lignocellulosic biomass. Appl. Energy 184, 548–559. https://doi.org/10.1016/j.apenergy.2016.10.039

Alibaba, 2021. Liquid Mixer agitator. https://thai.alibaba.com/product-detail/flow-acceleration-submersible-mixers-biogas-digesters-biogas-post-digesters-1600103512973.html?spm=a2700.details.0.0.48083ecfZqoXMd (accessed 10.8.21).

APHA., 2012. Standard methods for the examination of water and wastewater, 22th ed. Washington DC. USA.

Angelidaki, I., Sanders, W., 2004. Assessment of the anaerobic biodegradability of macropollutants. Rev. Environ. Sci. Biotechnol. 3, 117–129.

https://doi.org/10.1007/s11157-004-2502-3

Arreola-Vargas, J., Flores-Larios, A., González-Álvarez, V., Corona-González, R.I., Méndez-Acosta, H.O., 2016. Single and two-stage anaerobic digestion for hydrogen and methane production from acid and enzymatic hydrolysates of Agave tequilana bagasse. Int. J. Hydrogen Energy 41, 897–904. https://doi.org/10.1016/j.ijhydene.2015.11.016

Baldinelli, A., Barelli, L., Bidini, G., 2018. On the feasibility of on-farm biogas-to-electricity conversion: To what extent is solid oxide fuel cells durability a threat to break even the initial investment? Int. J. Hydrogen Energy 43, 16971–16985. https://doi.org/10.1016/j.ijhydene.2018.02.031

Chaiprapat, S., Wongchana, S., Loykulnant, S., Kongkaew, C., Charnnok, B., 2015. Evaluating sulfuric acid reduction, substitution, and recovery to improve environmental performance and biogas productivity in rubber latex industry. Process Saf. Environ. Prot. 94, 420–429. https://doi.org/10.1016/j.psep.2014.10.002

Chungchaichana, P., Vivanpatarakij S., 2012. Potential analysis of fresh-food market waste for biogas production to electricity; case study Talad-Thai. J. Energy Res. 9, 73-83.

Danwanichakul, P., Pohom, W., Yingsampancharoen, J., 2019. L-Quebrachitol from acidic serum obtained after rubber coagulation of skim natural rubber latex. Ind. Crops Prod. 137, 157–161. https://doi.org/10.1016/j.indcrop.2019.04.072

De Gioannis, G., Muntoni, A., Polettini, A., Pomi, R., Spiga, D., 2017. Energy recovery from one- and two-stage anaerobic digestion of food waste. Waste Manag. 68, 595–602. https://doi.org/10.1016/j.wasman.2017.06.013

722 Demirel, B., Yenigün, O., 2002. Two-phase anaerobic digestion processes: A review. J.
723 Chem. Technol. Biotechnol. 77, 743–755. https://doi.org/10.1002/jctb.630
724 Department of Alternative Energy Development and Efficiency, 2013. Information
725 Center for Study Research Project of Prototype Community Enterprise Green
726 Energy from Energy Plants (Biogas from Energy Plants) :Investment Guide for
727 Biogas Power Plants from Energy Plants.
728 http://webkc.dede.go.th/testmax/sites/default/
729 files/%E0%B8%84%E0%B8%B9%E0%B9%88%E0%B8%A1%E0%B8%B7%E0
730 %B8%AD%E0%B8%81%E0%B8%B2%E0%B8%A3%E0%B8%A5%E0%B8%8
731 7%E0%B8%97%E0%B8%B8%E0%B8%99%E0%B9%82%E0%B8%A3%E0%B
732 8%87%E0%B9%84%E0%B8%9F%E0%B8%9F%E0%B9%89%E0%B8%B2%E
733 0%B8%81%E0%B9%8A%E0%B8%B2%E0%B8%8B%E0%B8%8A%E0%B8%
734 B5%E0%B8%A7%E0%B8%A0%E0%B8%B2%E0%B8%9E%E0%B8%88%E0
735 %B8%B2%E0%B8%81%E0%B8%9E%E0%B8%B7%E0%B8%8A%E0%B8%9
736 E%E0%B8%A5%E0%B8%B1%E0%B8%87.pdf (accessed 15.8.21).
737 Feng, L., Gao, Y., Kou, W., Lang, X., Liu, Y., Li, R., Yu, M., Shao, L., Wang, X., 2017.
738 Application of the initial rate method in anaerobic digestion of kitchen waste.
739 Biomed Res. Int. 2017. https://doi.org/10.1155/2017/3808521
740 Gustavsson, J., Yekta, S.S., Sundberg, C., Karlsson, A., Ejlertsson, J., Skyllberg, U.,
741 Svensson, B.H., 2013. Bioavailability of cobalt and nickel during anaerobic
742 digestion of sulfur-rich stillage for biogas formation. Appl. Energy 112, 473–477.
743 https://doi.org/10.1016/j.apenergy.2013.02.009
744 Han, W., Hu, Y.Y., Li, S.Y., Li, F.F., Tang, J.H., 2016. Biohydrogen production from
745 waste bread in a continuous stirred tank reactor: A techno-economic analysis.

Bioresour. Technol. 221, 318–323. https://doi.org/10.1016/j.biortech.2016.09.055

Jariyaboon, R., O-Thong, S., Kongjan, P., 2015. Bio-hydrogen and bio-methane potentials of skim latex serum in batch thermophilic two-stage anaerobic digestion. Bioresour. Technol. 198, 198–206. https://doi.org/10.1016/j.biortech.2015.09.006

Kavitha, S., Yukesh Kannah, R., Yeom, I.T., Do, K.U., Banu, J.R., 2015. Combined thermo-chemo-sonic disintegration of waste activated sludge for biogas production. Bioresour. Technol. 197, 383–392. https://doi.org/10.1016/j.biortech.2015.08.131

Kongjan, P., Jariyaboon, R., O-Thong, S., 2014. Anaerobic digestion of skim latex serum (SLS) for hydrogen and methane production using a two-stage process in a series of up-flow anaerobic sludge blanket (UASB) reactor. Int. J. Hydrogen Energy 39, 19343–19348. https://doi.org/10.1016/j.ijhydene.2014.06.057

Kongjan, P., Sama, K., Sani, K., Jariyaboon, R., Reungsang, A., 2018. Feasibility of bio-hythane production by co-digesting skim latex serum (SLS) with palm oil mill effluent (POME) through two-phase anaerobic process. Int. J. Hydrogen Energy 43, 9577–9590. https://doi.org/10.1016/j.ijhydene.2018.04.052

Kreng thai wattana, 2021. Submersible pump (waste water). https://www.ktw.co.th/ (accessed 12.8.21).

Liu, Z., Zhang, C., Lu, Y., Wu, X., Wang, Lang, Wang, Linjun, Han, B., Xing, X.-H., 2013. States and challenges for high-value biohythane production from waste biomass by dark fermentation technology. Bioresour. Technol. 135, 292–303. https://doi.org/10.1016/j.biortech.2012.10.027

Lyberatos, G., Pullammanappallil, P.C., 2010. Anaerobic digestion in suspended growth bioreactors, in: Environmental Biotechnology. Springer, pp. 395–438.

DOI:10.1007/978-1-60327-140-0_9

Massanet-Nicolau, J., Dinsdale, R., Guwy, A., Shipley, G., 2013. Use of real time gas production data for more accurate comparison of continuous single-stage and two-stage fermentation. Bioresour. Technol. 129, 561–567. https://doi.org/10.1016/j.biortech.2012.11.102

Mu, T., Xing, J., Yang, M., 2019. Sulfate reduction by a haloalkaliphilic bench-scale sulfate-reducing bioreactor and its bacterial communities at different depths. Biochem. Eng. J. 147, 100–109. https://doi.org/10.1016/j.bej.2019.04.008

Nathao, C., Sirisukpoka, U., Pisutpaisal, N., 2013. Production of hydrogen and methane by one and two stage fermentation of food waste. Int. J. Hydrogen Energy 38, 15764–15769. https://doi.org/10.1016/j.ijhydene.2013.05.047

Nguyen, D.D., Jeon, B.H., Jeung, J.H., Rene, E.R., Banu, J.R., Ravindran, B., Vu, C.M., Ngo, H.H., Guo, W., Chang, S.W., 2019. Thermophilic anaerobic digestion of model organic wastes: Evaluation of biomethane production and multiple kinetic models analysis. Bioresour. Technol. 280, 269–276. https://doi.org/10.1016/j.biortech.2019.02.033

Patterson, T., Esteves, S., Dinsdale, R., Guwy, A., 2011. An evaluation of the policy and techno-economic factors affecting the potential for biogas upgrading for transport fuel use in the UK. Energy policy. 39, 1806-1816. https://doi.org/10.1016/j.enpol.2011.01.017.

Rajendran, K., Mahapatra, D., Venkatraman, A.V., Muthuswamy, S., Pugazhendhi, A., 2020. Advancing anaerobic digestion through two-stage processes: Current developments and future trends. Renew. Sustain. Energy Rev. 123, 109746. https://doi.org/10.1016/j.rser.2020.109746

794 Raketh, M., Jariyaboon, R., Kongjan, P., Trably, E., Reungsang, A., Sripitak, B.,
795 Chotisuwan, S., 2021. Sulfate removal using rubber wood ash to enhance biogas
796 production from sulfate-rich wastewater generated from a concentrated latex
797 factory. Biochem. Eng. J. 173, 108084. https://doi.org/10.1016/j.bej.2021.108084
798 Reungsang A., 2019. Thailand:Microbial-Derived Biofuels and Biochemicals, first ed.
799 Khon Kaen University, Thailand.
800 Rubber Intelligence Unit, 2018. Rubber in Thailand. http://rub ber.oie.go.th/ (accessed
801 25.4.18).
802 Sani, K., Kongjan, P., Pakhathirathien, C., Cheirsilp, B., O-Thong, S., Raketh, M.,
803 Kana, R., Jariyaboon, R., 2021. Effectiveness of using two-stage anaerobic
804 digestion to recover bio-energy from high strength palm oil mill effluents with
805 simultaneous treatment. J. Water Process Eng. 39, 101661.
806 https://doi.org/10.1016/j.jwpe.2020.101661
807 Schievano, A., Tenca, A., Scaglia, B., Merlino, G., Rizzi, A., Daffonchio, D., Oberti, R.,
808 Adani, F., 2012. Two-stage vs single-stage thermophilic anaerobic digestion:
809 Comparison of energy production and biodegradation efficiencies. Environ. Sci.
810 Technol. 46, 8502–8510. https://doi.org/10.1021/es301376n
811 Siripatana, C., Jijai, S., Kongjan, P., 2016. Analysis and extension of Gompertz-type and
812 Monod-type equations for estimation of design parameters from batch anaerobic
813 digestion experiments, in: AIP Conference Proceedings. AIP Publishing LLC, p.
814 30079. https://doi.org/10.1063/1.4965199
815 Sritrakul, N., (Master thesis) 1995. Pre-Feasibility Study on The System Design for Self
816 Drying Biogas-Sludge: A Case Study on Large Scale Livestock (Pigs) Farmming in
817 Nakhon Pathom Provience. Mahidol University, Thailand (in Thai).

Vo, T.T.Q., Wall, D.M., Ring, D., Rajendran, K., Murphy, J.D., 2018. Techno-economic analysis of biogas upgrading via amine scrubber, carbon capture and ex-situ methanation. Appl. Energy 212, 1191–1202. https://doi.org/10.1016/j.apenergy.2017.12.099

Wang, S., Yuan, R., Liu, C., Zhou, B., 2020. Effect of Fe2+ adding period on the biogas production and microbial community distribution during the dry anaerobic digestion process. Process Saf. Environ. Prot. 136, 234–241. https://doi.org/10.1016/j.psep.2019.12.031

Wang, Y., Zhang, Y., Wang, J., Meng, L., 2009. Effects of volatile fatty acid concentrations on methane yield and methanogenic bacteria. Biomass and Bioenergy 33, 848–853. https://doi.org/10.1016/j.biombioe.2009.01.007